
3-5 Geomagnetic Storms

NAGATSUMA Tsutomu

Geomagnetic storms, in which the global geomagnetic field intensity decreases on the order of tens to hundreds nT, are phenomena that occur on the largest scale in the solar wind-magnetosphere-ionosphere coupled system. Geomagnetic storms develop when solar wind-magnetosphere couplings are intensified by solar wind disturbances (coronal holes and CME phenomena) that accompany southward IMF. Perturbations in the magnetic field are caused by geomagnetic storms and can be explained by the westward electric current along the geomagnetic equator (ring current). Such perturbations on the scale of 10^{15} - 10^{16} J occur when the magnetosphere responds to the injections of energy during geomagnetic storms.

Geomagnetic storms are generally believed to develop in association with an increase in magnetospheric convection. However, in contrast to magnetospheric convection development (which is saturated with strong solar wind electric fields), analysis of the correlation of solar wind parameters to magnetospheric convection and to geomagnetic storms has revealed that geomagnetic storm growth is not saturated with such electric fields. This indicates that geomagnetic field growth and magnetospheric convection growth may not correlate perfectly.

Keywords

Geomagnetic storms, Solar wind-magnetosphere coupling, Magnetospheric convection, Ring current, Substorm

1 Introduction

The largest known disturbances in the solar wind-magnetosphere-ionosphere coupled system, geomagnetic storms are characterized by a prolonged period in which the horizontal component of geomagnetic fields is depressed in the mid to low latitudes on a global scale, with such periods lasting from one-half to several days. This paper examines the characteristics of a geomagnetic storm and the cause of its development, as well as prospects for future research.

2 Features of Geomagnetic Variations

The Earth has an internal magnetic field generated by the dynamo effects of electric

currents in its fluid outer core. Couplings between this internal magnetic field and the solar wind form the magnetosphere, which has a comet-like shape, with a tail extending away from the Sun. Variations in solar wind-magnetosphere couplings serve as the driving force behind various characteristic geomagnetic disturbances. Although components of the geomagnetic field variation can be attributed to the internal dynamo effect, their periods are much longer than the periods of variations caused by solar wind-magnetosphere couplings, and can be regarded as a separate phenomenon.

During quiet periods free of geomagnetic disturbances, the geomagnetic field displays a relatively regular pattern of variation. These regular variations are caused by ionospheric currents generated by the dynamo effect aris-

ing from the tidal motion of the thermosphere.

The tidal motion of the thermosphere is driven by heat energy from the Sun.

Geomagnetic disturbances generally fall into two broad categories. The first involves variations in the horizontal geomagnetic field component in the polar region in the range of several hundred to one thousand and several hundred nT, occurring on time scales of 30 minutes to 2 hours. These variations correspond to geomagnetic field perturbations called "substorms." Optically, a substorm is defined as a phenomenon that begins with an explosive illumination of the aurora near the midnight region on the nightside that gradually expands both in the longitudinal and latitudinal directions. The changes observed in the geomagnetic field accompanying substorms differ significantly for different magnetic local times and magnetic latitudes. Furthermore, the effects of a substorm may appear as bay-like geomagnetic field variations in the low to middle latitudes on the nightside.

The second type of geomagnetic disturbance involves a prolonged depression of the horizontal geomagnetic field component in the mid to low latitudes in the range of several tens to several hundred nT that lasts from one-half to several days. This type of disturbance is called a "geomagnetic storm." The period of progressive depression of field strength is called the "main phase." The period of restoration to original field strength is called the "recovery phase." A geomagnetic storm may accompany a "sudden commencement (SC)," characterized by a sudden increase in the magnetic field intensity shortly before the main phase. The period between the sudden commencement and main phase is called the "initial phase." A geomagnetic storm not accompanied by a SC is called a "gradual geomagnetic storm (SG)." Fig.1 shows an example of SC- and SG-type geomagnetic storms observed at the Kakioka Geomagnetic Observatory. The SC is a geomagnetic perturbation caused by an increase in magnetopause currents due to the rapid compression of the magnetosphere by the dynamic pressure of the

solar wind, which is intensified by interplanetary shock.

However, in certain cases, interplanetary shock does not trigger geomagnetic storms. In other words, geomagnetic perturbations during the main and recovery phases are the essential features of a geomagnetic storm. These two phases are believed to be essentially identical in both SC and SG storm types. Substorms also frequently occur during geomagnetic storms, and the superposition of corresponding short-period geomagnetic perturbations onto those of geomagnetic storms results in a complex pattern of variations.

The degree of depression of the horizontal geomagnetic field component observed during geomagnetic storms differs, depending on the magnetic local time. The maximum depression of the geomagnetic field strength is seen on the night to dusk side, while the minimum depression is seen on the day to dawn side. This is due to the asymmetrical flow of the ring current, which will be explained in a later section.

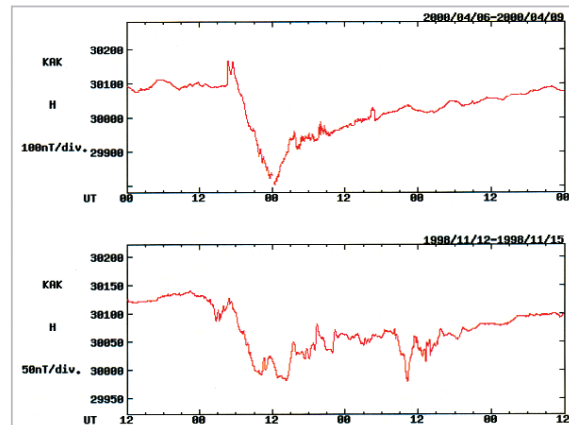


Fig.1 Examples of geomagnetic storms for sudden commencement (SC) type (top panel) and gradual (SG) type (bottom panel)

3 Solar Wind Variations and Geomagnetic Storms

Geomagnetic disturbances are driven by solar wind-magnetosphere couplings. Solar wind energy is injected into the magnetosphere through field line merging of the inter-

planetary magnetic field (IMF) and geomagnetic field. This energy injection is most efficient during southward IMF (B_s component). Prolonged periods of strong southward IMF will trigger geomagnetic storms. Observations have shown that a state of $B_s \geq 10$ nT lasting for over 3 hours will always generate a geomagnetic storm[1]. Solar wind velocity (V) is another important factor. Geomagnetic storm development is known to demonstrate a strong positive correlation with the product of these two physical quantities, VBs.

Two types of solar surface phenomena are believed to generate high VBs conditions:

coronal mass ejection (CME) and coronal holes. CMEs are a phenomenon in which large amounts of solar coronal plasma is released into interplanetary space (Fig.2). CMEs appear simply as a region of high plasma density, but may contain a magnetic flux rope structure[2].

The magnetic flux rope has a stable magnetic field structure. When the structure contains a stable southward magnetic field component, it is a significant driver of geomagnetic storms.

This structure also generates an interplanetary shock before the CME, helping to devel-

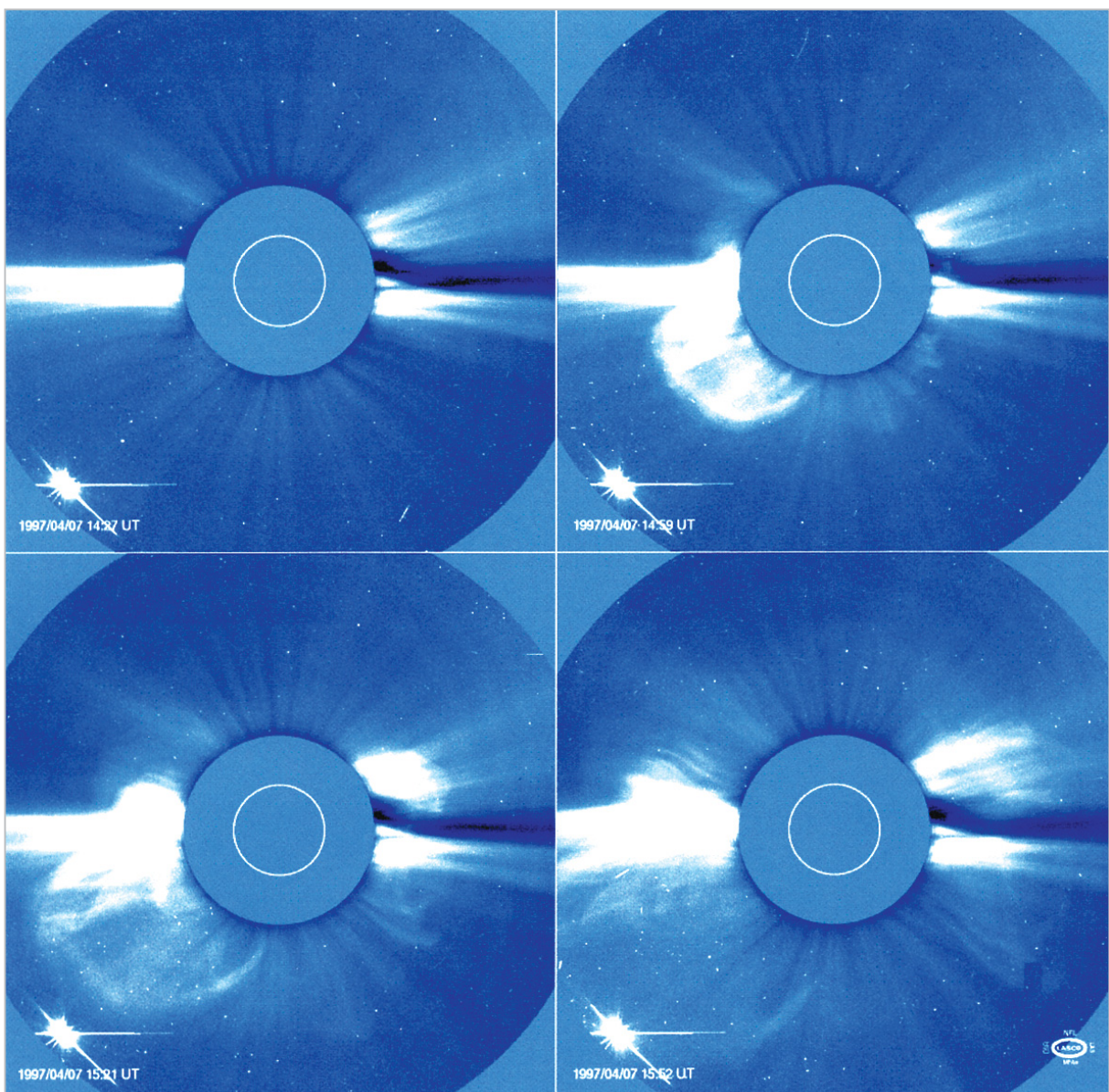


Fig.2 CME observed by coronagraph (LASCO) aboard the SOHO satellite (ESA & NASA)

op geomagnetic storms when the magnetic field in the sheath region has a southward component.

Coronal holes are areas in which high-speed solar winds stream out from the Sun.

Coronal holes have weak solar magnetic fields compared to active regions and form in regions having the same polarity over a wide area (unipolar magnetic fields). Such regions have lower coronal plasma temperatures than surrounding regions, and hence, appearing for this reason to be relatively dark (Fig.3). The high-speed solar winds ejected from coronal holes overtake and interact with low-speed solar wind in its path, creating a co-rotating interaction region (CIR). Within the CIR, plasma pressure is increased by compression.

Magnetic field strength also increases. When the southward component is dominant in the strengthened magnetic field, its interactions with the geomagnetic field are strengthened, driving a geomagnetic storm.

Since CMEs are sporadic, geomagnetic storms associated with them are sometimes called "sporadic geomagnetic storms." On the other hand, the structure of a coronal hole may sometimes remain relatively stable through several periods of solar rotation. In such cases, a recurrent CIR is observed from the Earth, with cycles equivalent to the rotational periods of the Sun. If the CIR has a dominant southward magnetic field component, "recurrent geomagnetic storms" are generated. In addition to above case, recurrent geomagnetic

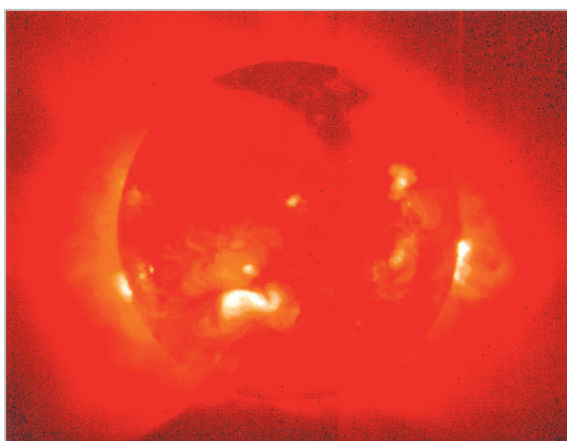


Fig.3 Coronal hole observed by the Yohkoh satellite (courtesy of ISAS)

storms may also be generated when CMEs occur often in a specific active region on the Sun over several rotational periods. If a strong southward magnetic field is produced by interactions between a high-speed solar wind and CME, even stronger geomagnetic storms are triggered.

4 Geomagnetic Storm Indices

Used as an indicator of the magnitude of a geomagnetic storm, the Dst index is based on geomagnetic data at middle latitudes, with ranges stretching in the meridional direction collected at four stations (Kakioka, Hermanus, San Juan, and Honolulu), and is expressed as the hourly value indicating the degree of variation in the symmetrical component[3]. The locations of the geomagnetic observatories are shown in Fig.4. The Dst index is calculated by assuming that the intensity of a geomagnetic storm can be represented equivalently by the scale of the symmetric current flowing westward at the equator, called the ring current. The details of the ring current will be discussed in the next section. The actual Dst index is known to contain components of geomagnetic field variations in the magnetopause current and in the tail currents, which are imposed on variations of the ring current. The Dst index corrected for the effects of magnetopause current is called the pressure corrected Dst index (Dst* index), and is defined by the following equation[4]:

$$Dst^* = Dst - b \times P_{sw}^{0.5} + c \quad (1)$$

where P_{sw} is the solar wind dynamic pressure (ρV^2) [nPa]. Values for b and c are determined from analysis. Various values have been proposed according to different models. However, all proposed values are approximately equal. (For example, $b = 7.26$ [nT(nPa)^{-1/2}] and $c = 11$ [nT][5].) The extent of the contribution from the tail current is still being disputed, and no correction method has been established.

The relationship between the Dst* index and the total energy of the ring current parti-

cles can also be approximated by the Dessler-Parker-Scopke relation below[6][7].

$$\frac{Dst^*}{B_0} = \frac{2E_{\perp}}{3E_M} \quad (2)$$

where B_0 is the geomagnetic field strength at the Earth's surface and $2E_{\perp}$ and E_M , are the total energy of the ring current particles and the Earth's external magnetic field. This equation shows that the Dst^* index is an indicator for the total energy stored within the magnetosphere in the form of the ring current. Thus, a geomagnetic storm can be considered a state in which a large amount of energy accumulates within the magnetosphere. This equation indicates that total energy during a geomagnetic storm (energy of the geomagnetic storm) is on the order of 10^{15} - 10^{16} J.

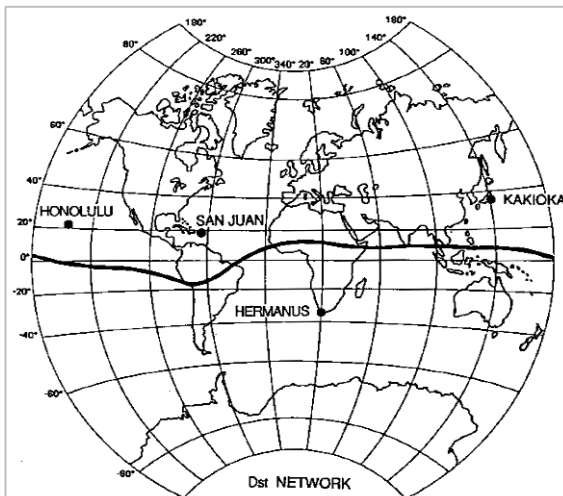


Fig.4 Locations of the geomagnetic observatories used to determine the Dst index[3]

5 The Ring Current

The depression of the geomagnetic field during geomagnetic storms can be explained by the effects of the dominating symmetric westward electric current at the equator, which flows in the region of 2-9 Re (Earth radii), called the ring current. Development of this current is thought to be promoted by solar wind-magnetosphere couplings. Convection driven by the dayside merging of the solar wind and geomagnetic field lines transports plasma and magnetic flux to the magnetotail.

The plasma and magnetic flux are then transported from the tail to the interior region of the magnetosphere (inner magnetosphere) through magnetic reconnection of the distant-tail neutral lines. As convection accelerates, the plasma is transported further inwards. In a steady state ($dv/dt=0$), the pressure gradient of the plasma and the Lorentz force ($J \times B$) is in equilibrium in the magnetospheric convection[8]. In the inner magnetosphere, the plasma pressure gradient and the Lorentz force by the ring current are balanced.

The pressure distribution within the plasma depends on state of geomagnetic activity.

On average, the plasma pressure peaks at approximately 3 Re , with gradients decreasing in the Earthward and anti-Earthward directions away from the peak. Therefore, if it is assumed that the plasma pressure gradient is in balance with $J \times B$, the electric current flows westward in the anti-Earthward region from the peak, and eastward in the Earthward region from the peak. As a result, the decrease in total geomagnetic force is more marked near the peak of the plasma pressure than at the Earth's surface.

In Fig.5, the changes in Dst indices observed for a geomagnetic storm on June 4-6, 1991 are shown as a solid line, while changes in ΔB at the geomagnetic equator at approximately 2.5 Re observed by the Akebono satellite during the corresponding time period are shown as solid black dots. The Akebono satellite, a magnetosphere exploration satellite launched in Feb. 1989 by the ISAS, has made observations during the time period indicated in Fig.5 at the geomagnetic equator at approximately 2.5 Re at MLT near midnight. ΔB is the difference in total magnetic force observed by satellite and estimated by the International Geomagnetic Reference Field (IGRF), one of the standard models representing the Earth's internal magnetic field. In approximation, it corresponds to the change in magnetic field caused by the ring current at the position of the satellite. The most obvious feature of this plot is the difference of approximately 50 nT between ΔB and Dst indices in

the quiet period, which is believed to result from the effect of the ring current flowing during the quiet period. Results of past satellite observations have shown that even when geomagnetic fields are quiet, magnetic field is suppressed near 2.5 Re by approximately -30 nT to -50 nT, compared to the model magnetic field. This suppression is greatest on the dusk side and weakest on the dawn side[9]. When the effects of the ring current during the quiet period are subtracted, the trend of changes in ΔB generally corresponds to that of Dst indices.

However, near 6:00 UT and 18:00 UT, when the main phase of the geomagnetic storm progresses rapidly, it can be seen that the ΔB is more than 200 nT lower than the Dst indices.

The large decrease observed in ΔB relative to Dst implies that the peak position of the plasma pressure in the inner magnetosphere had reached the vicinity of the Akebono satellite during the development of the main phase.

Since ions are the dominant sources in determining plasma pressure, ring currents can be said to consist mainly of ions. Normally, the magnetosphere consists predominantly of protons (hydrogen ions). However, the ratio of oxygen ions within the magnetosphere may increase significantly during large geomagnetic storms[10]. These oxygen ions are believed to originate in the ionosphere. However, the energy of ions in the ionosphere is only on the order of several eV, while that of the ions in the ring current is on the order of several keV to several ten keV. Clearly, some mechanism not clearly understood at present heats and accelerates the ionospheric ions to energy levels seen in the ring current during geomagnetic storms.

The dissipation of the ring current is thought to be caused by charge-exchange process with the geocorona, Coulomb scattering with the thermal plasma of the plasmasphere, and pitch angle scattering due to interactions with the plasma wave. It is known that in some cases, the magnetic field recovers in two stages: rapidly at the beginning of the

recovery phase of a geomagnetic storm, and gradually thereafter. It has been suggested that this may be due to the effects of a shorter decay constant for oxygen ions than protons for charge-exchange reaction, or due to the effects of loss at the dayside magnetopause by convection.

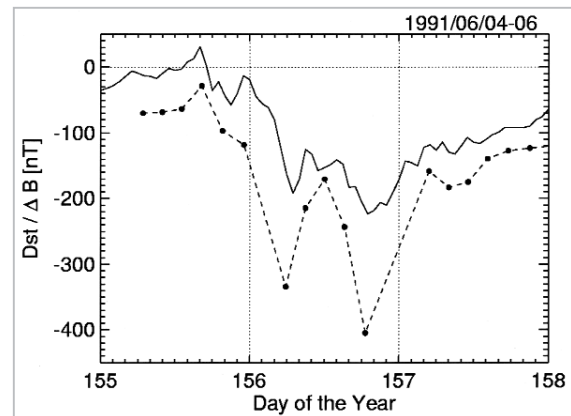


Fig.5 The changes in Dst indices during a geomagnetic storm on June 4-6, 1991 and changes in ΔB observed at the geomagnetic equator ($L = 2.5$ Re) near midnight region by the Akebono satellite

6 Particle Drift

Plasma motion in the external magnetosphere can be modeled as a magnetohydrodynamics (MHD), after which the phenomena can be reconstructed by global MHD simulations. On the other hand, the inner magnetosphere in which the ring current develops has a small β value ($p/(B^2/2\mu_0)$) and large gradients in both the geomagnetic field strength and curvature. In this region, the effects upon particle transport of gradient drift and curvature drift by the magnetic field becomes dominant, along with that of the $E \times B$ drift.

Since ideal MHD can only be applied to plasma motion by the $E \times B$ drift, it cannot be used to express plasma motion accurately in the inner magnetosphere[11]. The previous section discussed the ring current within a MHD framework. For a more precise examination, particle kinetic effects must also be considered. Here, we will examine particle motion in the inner magnetosphere.

The gradient drift W_G and curvature drift W_C can be described as follows:

$$W_G = (mv_{\perp}^2/2qB^3) (B \times \nabla B)/B^3 \quad (3)$$

$$W_C = (mv_{\parallel}^2/qB^4)(B \times (B \cdot \nabla)B)/B^4 \quad (4)$$

Here, v_{\perp} and v_{\parallel} are velocities perpendicular and parallel to magnetic field lines, while q is electric charge. Gradient drift is enhanced closer to the Earth. Plasma transported from the magnetotail by the $E \times B$ drift is more strongly affected by gradient drift as it approaches the Earth, as a result of which ions are transported duskward, while electrons are transported dawnward, both being kept from further approaching the Earth. The point at which the $E \times B$ drift velocity equals gradient drift velocity is considered to indicate the particle penetration limit (Fig.6). It can be seen that particles penetrate deeper into the Earth's vicinity when the applied electric field is stronger. The penetration limit also depends on particle energy. The region further within the particles' penetration limit is called the Alfvén layer.

Since the centers of gyration (guiding center) of electrons and ions move in the opposite direction in the cases of gradient and curvature drifts, a drift current is generated.

The gradient drift current J_G and the curvature drift current J_C are expressed as follows:

$$J_G = P_{\perp}(B \times \nabla B)/B^3 \quad (5)$$

$$J_C = P_{\parallel}(B \times (B \cdot \nabla)B)/B^4 \quad (6)$$

where P_{\perp} and P_{\parallel} are plasma pressures perpendicular and parallel to the magnetic field lines, respectively.

A magnetization current J_m generated by non-uniform spatial distribution of the particles' magnetic moment is given by the following equation[12]:

$$J_m = (B/B^2) \times \nabla P_{\perp} - P_{\perp}(B \times (B \cdot \nabla)B)/B^4 - P_{\perp}(B \times \nabla B)/B^3 \quad (7)$$

The current perpendicular to the magnetic field line J_{\perp} can be expressed as the sum of the drift current and the magnetization current.

$$\begin{aligned} J_{\perp} &= J_m + J_G + J_C \\ &= (B/B^2) \times \nabla P_{\perp} + (P_{\parallel} - P_{\perp}) (B \times (B \cdot \nabla)B)/B^4 \quad (8) \end{aligned}$$

When the pressures parallel and perpendicular to the magnetic field lines are equal, only the effect of the magnetization current remains, and J_{\perp} is equivalent to that obtained from the MHD formula. If an isotropic pressure distribution can be assumed, the balance of force can be discussed within a MHD framework. We also see that the gradient drift and part of the magnetization current cancel each other out, so that the effect of the former is not apparent. Gradient drift transports ions to the dusk side and electrons to the dawn side in the inner magnetosphere, but these particle motions do not generate an electric current. But since ions contribute significantly to plasma pressure, the asymmetrical transport of electrons and ions results in a dawn-dusk asymmetry in the pressure gradient, which in turn creates a dawn-dusk asymmetry in the ring current. When the magnetospheric electric field is increasing, an asymmetry is created in the ring current. When the development of the electric field terminates and particle injection stops, particle motion in the inner magnetosphere assumes a closed orbit, and the ring current recovers its symmetry.

Although the opposing motions of ions and electrons may appear to result in the accumulation of positive and negative charges on the dusk and dawn sides, respectively, the charges are quickly canceled out by plasma supplied from the ionosphere. Thus, they do not accumulate. Except in an unsteady state, such charge accumulation is not considered to play an essential role in the development of convection and geomagnetic storms. If they do not cancel out, the polarization electric field produced by the motions of ions and electrons promotes changes in particle drift motion, and the state of particle distribution actually observed in the magnetosphere is unstable. Note that the above equations for drift current and magnetization current assume a condition of motion within a static magnetic field; the effects of the secondary electric field generated by the motions of ions and electrons are not considered.

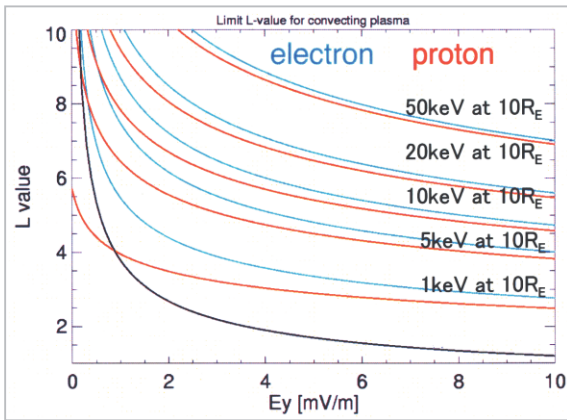


Fig.6 Penetration limit of particles transported from the magnetotail by convection

7 Geomagnetic Storm (Dst Index) Prediction

If the Dst^* index is considered to be an indicator for total particle energy stored within the magnetosphere, the growth and decay in Dst^* values can be expressed by an equation of balance between energy injection and decay[4]:

$$\frac{dDst^*}{dt} = Q(t) - \frac{Dst^*}{\tau} \quad (9)$$

Here, $Q(t)$ is the rate of energy injection, while τ is the decay constant. The second term on the right-hand side of the equation (decay term) takes this form because the Dst tends to decay exponentially during the recovery phase.

Numerous past studies have attempted to predict the Dst index by defining $Q(t)$ as a function of the solar wind parameter and by assuming a value for τ . Although various input parameters for solar wind have been proposed, results of statistical analysis of long-term solar wind data have shown that VBs is the parameter that most closely reconstructs observed variations in Dst [5][13]. Models assuming a constant decay constant or ones dependent on the value of Dst index have been the ones most widely used[14]. For example, Burton's model[4] assumes $\tau = 7.7$ [hour].

A model recently proposed defines the decay constant as a function of VBs when $Q(t)$ is defined as a function of VBs, based on the

assumption that the main process of decay is the charge exchange between the ring current ions and the geocorona[5]. Since the density of the geocorona increases exponentially towards the Earth, the decay constant for the charge exchange becomes shorter nearer to the Earth. If the magnetospheric plasma is transported closer to the Earth according to the value of VBs, the shortening of the decay constant of τ can be interpreted to be dependent on VBs as well. But note that the estimated magnitude of geomagnetic storms tends to be lower than the actual observed magnitude for storms with $Dst \leq -150$ nT when using this decay constant model.

Fig.7 compares the Dst^* indices predicted based on the O'Brien and McPherron model[5] (OM model) to those determined from observations, as well as Dst^* indices predicted based on the Burton model[4] (B model) to those determined from observations. Although the OM model has a high coefficient of correlation, predicted Dst^* values tend to be lower than the observed values for $Dst^* < -150$ nT. For larger geomagnetic storms, the B model sometimes appears to give more accurate predictions. To reconstruct large geomagnetic storms, we must increase the energy injection rate accompanying an increase in VBs, or to use longer decay constants than proposed by the OM model. As will be elaborated further below, it is difficult to imagine a condition in which only the energy injection rate increases, since the development of magnetospheric convection are saturated by the intense solar wind electric fields. On the other hand, the OM model defines τ , assuming that decay occurs only by the charge exchange process by the geocorona. In reality, Coulomb scattering and wave-particle interaction also contribute. The model adopted for τ must be examined further.

The energy injection rate due to increased numbers of particles injected into the magnetosphere cannot be ignored. However, it is difficult to determine a valid and universal decay constant, since the number of large geomagnetic storms occurrences is limited.

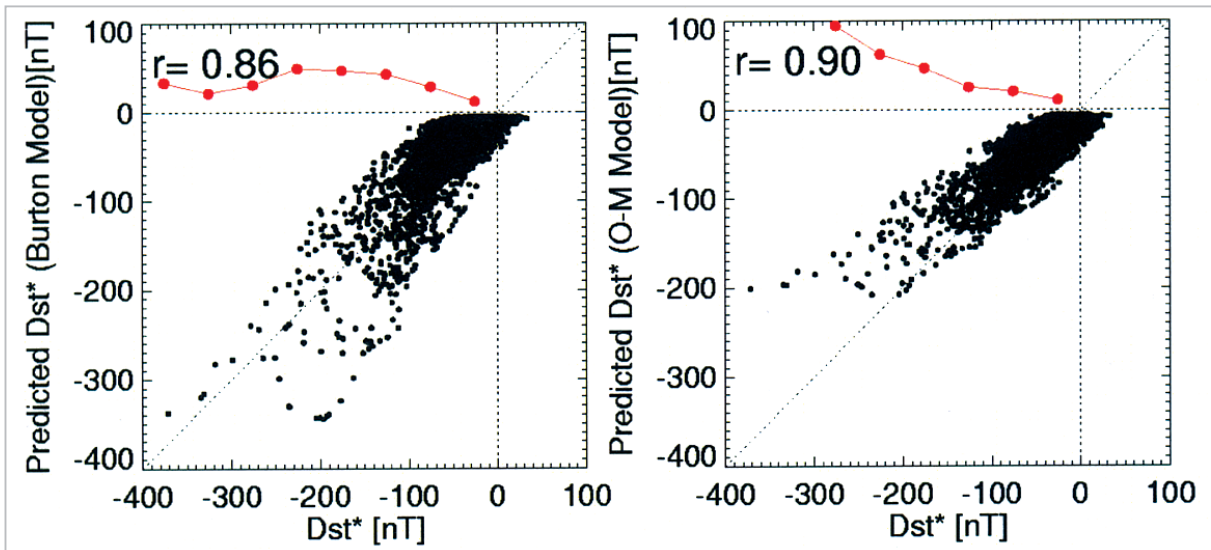


Fig.7 Observed and predicted Dst^* indices (Left: Burton's model (4); Right: O'Brien and McPherron model (5).)

A different approach to Dst index prediction uses neutral networks[15]. The correlations between solar wind data and Dst indices are catalogued and the results used to construct a neutral network model. This model is then used to predict Dst indices. The results have been found to be relatively accurate. However, certain difficulties arise in predictions with the arrival of solar wind variations of unknown patterns. The validation of results and the stability of the model need to be further examined.

8 Magnetospheric Convection During a Geomagnetic Storm

As stated earlier, a correlation has been confirmed by observation between geomagnetic storms and solar wind VBs. Since such positive correlation is also present during the growth of magnetospheric convection, it has been suggested that the growth of a magnetospheric convection may be the major factor behind geomagnetic storm growth[5][16].

While this may be true under normal solar wind conditions, the two have been found to behave differently when the solar wind electric field is intensified.

It has long been suggested that the magnetospheric convection driven by the solar wind-magnetosphere coupling may be a non-linear

coupling. One such possibility is the suppression of the reconnection efficiency of magnetic field lines when magnetic field strengths differ for the dayside magnetosphere and the IMF. In this case, the development of magnetospheric convection would be suppressed for strong IMF[17][18]. Another possibility is a decrease in magnetic reconnection efficiency due to changes in the dayside magnetopause magnetic field caused by the magnetic field generated by Region 1 field-aligned currents (FAC), which transfer the convection motion from the magnetosphere to the ionosphere. The development of magnetospheric convection can be expressed as the polar cap potentials calculated from the width of the convecting region and the electric field of the magnetosphere.

If the ionosphere has uniform conductivity, the current intensity of the Region 1 FAC is proportional to the polar cap potential. Thus, we can predict that the growth of magnetospheric convection will be suppressed for strong solar wind electric fields[19][20].

The PC index is an indicator representing the variation in the horizontal component of the geomagnetic field near the magnetic pole. It is known to correlate well with the solar wind electric field ($E_m = VB_T \sin^2(\theta/2)$), and can be used as an indicator for both the polar cap potential and the magnetospheric convec-

tion^{[21][22]}. PC index and solar wind parameters (E_m) have been used to investigate the response of the magnetospheric convection to strong solar wind electric fields. Fig.8 shows the results of statistical analysis of the PC index (PCN) of Qaanaaq (Thule), according to varying ranges of solar wind parameters (E_m). According to this analysis, the magnetospheric convection displays a clear non-linear effect, including a peak for $E_m \geq 5$ mV/m. Furthermore, it was found that this non-linear effect depends only on the intensity of the solar wind electric field, not on IMF strength. This supports the theory that the development of Region 1 currents suppresses magnetospheric convection^[23].

Are such non-linear effects seen for the Dst* index? According to Burton's model^[4], when an electric field with a maximum strength of 5 mV/m is applied to the magnetosphere, the maximum Dst* (geomagnetic storm) predicted assuming a steady field of 5 mV/m is around -190 nT. However, numerous geomagnetic storms on far larger scales have been observed in the past. As stated in the previous section, the Burton^[4] and the O'Brien and McPherron^[5] models, which assume that the energy influx from the solar wind to the magnetosphere increases linearly, have predicted geomagnetic storms with relative accuracy, including those with Dst* < -190 nT, although the problem of decay constants does remain.

This implies that the energy influx from the solar wind to the ring current increases linearly, behaving differently from the magnetospheric convection, which grows non-linearly. This throws some doubt on the theory that magnetospheric convection growth drives geomagnetic storm development.

Several observations suggest that the plasma is transported to the vicinity of the Earth during geomagnetic storms. The CRRES satellite has made direct observations of the electric field of the inner magnetosphere during the main phase of a geomagnetic storm, reporting electric fields of several mV/m in regions closer to the Earth than $L = 4$ ^[24].

However, the mechanism that generates such large electric fields (plasma flow) within the inner magnetosphere remains unclear. Given the limited numbers of satellites capable of making direct observations of the inner magnetosphere at this time, electric field measurements of the inner magnetosphere during geomagnetic storms remains an important research theme for the future.

Observations have also confirmed that the peak position of particle flux in the outer radiation belt moves inwards with the growth of a geomagnetic storm^[25]. The most widely supported theory at this time to explain the increase in flux near the peak in the outer radiation belt invokes the acceleration of electrons with energies of several 10 keV injected into the inner magnetosphere (internal acceleration theory). According to this theory, the plasma of several 10 keV must be transported further inwards, depending on the size of the geomagnetic storm. Such plasma transport would require a very large electric field.

If magnetospheric convection is not saturated, in contrast to saturated ionospheric convection, a gap will exist in the values of the polar cap potential at the ionosphere/magnetosphere boundary. As long as the magnetosphere and ionosphere are coupled, the difference in polar cap potentials on the ionosphere and the magnetosphere sides must be relieved as the difference in FAC potential. Calculations indicate that a FAC potential exceeding several 10 keV will be required. However, observations have yet to confirm the existence of such large FAC potential differences. Further study is required to clarify the mutual effects of plasma motions in the ionosphere and the magnetosphere.

On the other hand, perhaps the increase in solar wind density during geomagnetic storms leads to increased numbers of particles entering the magnetosphere, even when the rate of energy injection into the magnetosphere peaks and begins to decline due to the saturation of convection, increasing the energy accumulated in the form of the ring current.

Observations have demonstrated a correla-

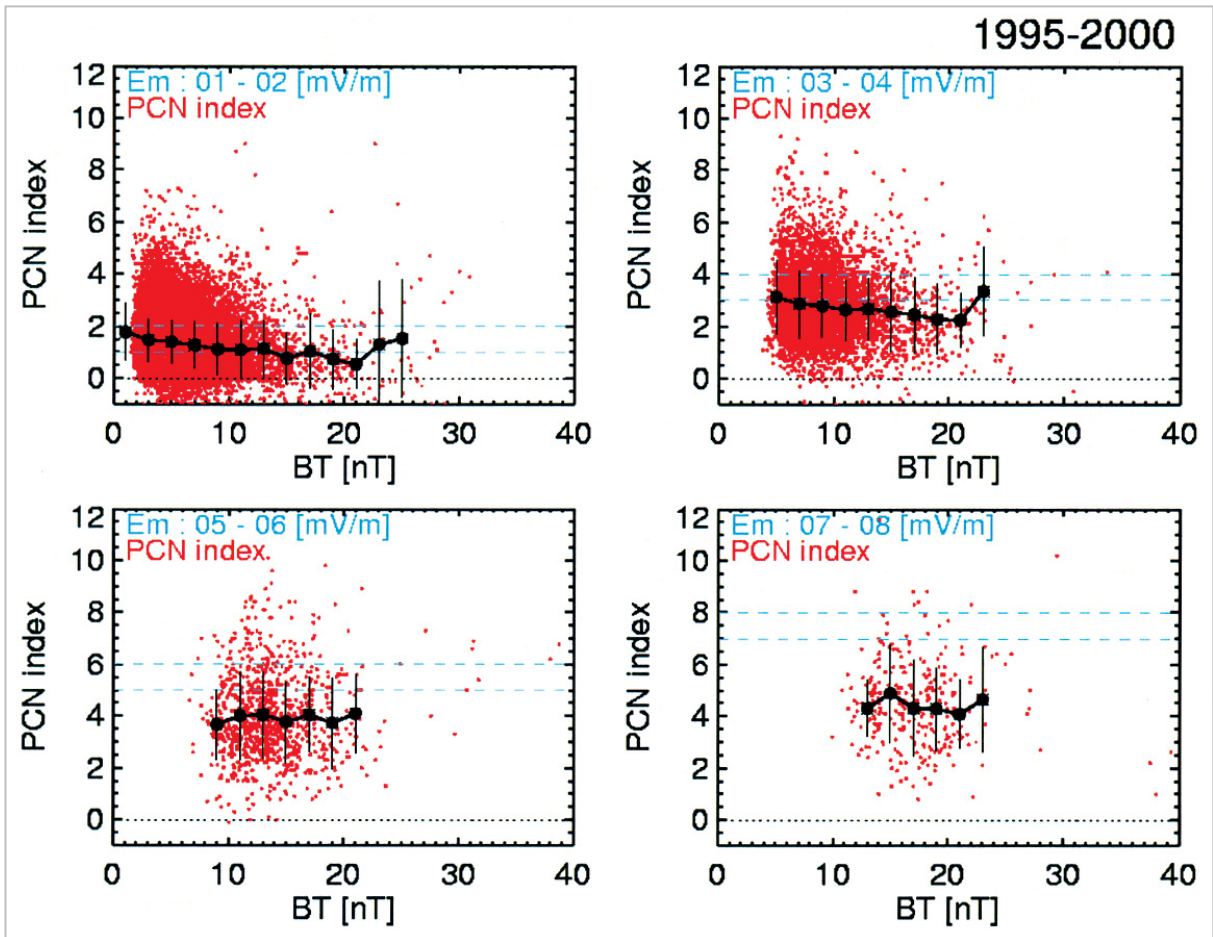


Fig.8 B_T dependence of PCN index for E_m of 1-2 mV/m (top left), 03-04 mV/m (top right), 05-06 mV/m (bottom left), and 07-08 mV/m (bottom right) [23]

tion between plasma sheet density and solar wind density[26][27], supporting this hypothesis. Furthermore, Dst indices calculated by particle tracing simulations that take plasma sheet density variations into consideration have been shown to agree quite well with observation[28]. However, note that particle tracing simulations can only reconstruct geomagnetic storms with Dst of -100 nT. It has been statistically shown that solar wind density variations have no dependency on geomagnetic storm developments[29].

9 Geomagnetic Storms and Substorms

A substorm was originally defined as a basic element of a geomagnetic storm (thus, termed "sub" storm)[30]. When substorms had first been defined, a working hypothesis that frequent occurrences of substorms leads to the

generation and development of a geomagnetic storm was proposed. It was generally believed that an understanding of substorms should lead to an understanding of geomagnetic storms. Now, it is clear that the relationship between substorms and geomagnetic storms is not so simple, and that they need to be considered as independent phenomena.

The frequent occurrence of substorms does not necessarily lead to geomagnetic storm development. Results of statistical comparisons of variations in geomagnetic storms and substorms using geomagnetic indices have shown that the growth of Dst index is suppressed during substorm development, or even converted to a recovery phase[31]. This suggests the possibility that substorms actually suppress the growth of Dst. On the other hand, some scientists view the recovery of the Dst index as only an apparent one arising from the decrease in the tail current, arguing that

the ring current itself may be developing, alongside the substorm[32].

The hypothesis of frequent substorms triggering geomagnetic storms attributes ring current growth to the injection of particles into the inner magnetosphere during substorms.

However, the results of imaging observations of the inner magnetosphere using energetic neutral atoms (ENA) demonstrate that particle injection accompanying substorms alone cannot account for the creation of the ring current[33].

Based on results of particle tracing simulations, it has also been reported that the decrease in Dst caused by particles injected by induced electric fields during a single substorm event is, at most, several nT[34].

Substorms occur frequently, even when geomagnetic storms are absent. The difference between substorms that trigger geomagnetic storms and those that do not are not clear. However, some researchers do claim to have found a difference between substorms associated with geomagnetic storms and those not so associated[35].

10 Prospects for Future Geomagnetic Storm Research (The Importance of Inner Magnetosphere Research)

The deployment of global observation networks both on ground and by satellite, together with the emergence of global MHD simulations, has advanced our understanding of the convection in the Earth's magnetosphere and substorms[8]. However, given the limited number of satellites that have made direct observations of the inner magnetosphere, many problems remain to be resolved by observation, especially with respect to the dynamics of the outer radiation belt. Since particle motion due to gradient and curvature drift in the magnetic field cannot be ignored, the extent of the understanding that may be achieved through ideal MHD simulations alone is limited. Numerous attempts have been made to reconstruct geomagnetic storms

through particle tracing simulations based on static magnetic field models. However, in the case of large geomagnetic storms with Dst dropping below -100 nT, the electric currents generated by injected particles would significantly affect the structure of the magnetic fields in their vicinity. Thus, the results of particle tracing simulations using a static magnetic field model are unlikely to reconstruct the actual state of geomagnetic storms. Although we must consider the non-linear effects of changes in magnetic field structures caused by injected particles, simulations have not yet been able to incorporate such effects. Additionally, the results of such simulations differ significantly depending on the magnetic and electric field models adopted. The author believes that a quantitative reconstruction of geomagnetic storms must ultimately await a full particle simulation capable of incorporating particle kinetic effects.

Direct satellite measurements of the inner magnetosphere are also important and must be made by multiple satellites (constellations), since temporal and spatial variations are not easily distinguishable in data from single satellite observations. In recent years, advances in ENA imaging technology have enabled 2-D imaging of the ring current.

Snapshots of plasma (ion) spatial distributions are now becoming available. In the future, satellite observation networks such as constellations for direct observation of the inner magnetosphere and ENA imaging constellations should be deployed to reveal, through observations, variations in plasma pressure distribution and changes in plasma flow (electric field distribution) in the inner magnetosphere and their various causal factors.

Appendix: The Effect of Geomagnetic Storms on Society

Geomagnetic storms are the largest-scale disturbances in the magnetosphere.

Large-scale variations produced in the space environment by this disturbance generate numerous hazards. One of the most important themes in space weather forecasting

is to gain a solid understanding of geomagnetic storms, to make accurate predictions and to provide advance warning of its effects. The following is an introduction to the space environment variations that accompany geomagnetic storms and the potential hazards that they present.

Ionospheric Storms and Thermospheric Expansion

During the growth of geomagnetic storms, convection in the magnetosphere is enhanced and substorms occur frequently. The ionospheric current in the polar region also gathers strength. The energy supplied to the polar region heats the thermosphere, which changes chemical compositions and generates large-scale motion in the thermosphere. Such conditions may lead to the generation of an ionospheric storm, which in turn may cause communication failures[36]. The heating and subsequent expansion of the thermosphere may significantly disturb the attitudes and orbits of satellites in low Earth orbit.

Geomagnetic Induced Currents

Geomagnetic storms may accompany sudden, short-period geomagnetic field variations. Sudden geomagnetic changes induce currents in power lines and pipelines. These induced currents may destroy power transmission systems and corrode pipelines. The threats posed by geomagnetic induced currents are widely acknowledged in polar regions, where strong ionospheric currents have been observed. However, recent observations have confirmed cases of strong currents induced in power lines during geomagnetic storms, even in middle to low latitude regions such as Japan[37].

Increase in Outer Radiation Belts Electron Flux

Variations in the relativistic electron flux in the outer radiation belt are deeply related to geomagnetic storms. Normally, during the growth of the main phase of the geomagnetic storm, the relativistic electron flux in the outer radiation belt decreases. Later in the recovery phase, the relativistic electron flux sometimes displays a significant increase relative to before the onset of the geomagnetic storm[38].

Relativistic electrons cause deep dielectric charges in electronic circuits within satellites. When flux increases, the probability of deep dielectric charges also increases, potentially leading to malfunctions and the failure of satellite instruments.

Expansion of the Region Affected by the Proton Event

The arrival of energetic protons accelerated by solar flares at the Earth is called a proton event. Proton events damage solar cell panels and increase radiation exposure of crew aboard spacecrafts and space stations. The precipitation of energetic protons in a proton event in the polar ionosphere may cause ionization anomalies leading to communication failures in the HF band, called polar cap absorptions (PCA). The precipitated protons also generate secondary cosmic rays, increasing the exposure of aircraft crew to radiation while traveling through polar regions. During quiet periods, the penetration of energetic particles are limited to polar caps by the shielding effect of the geomagnetic field. But during geomagnetic storms, the magnetic field structure of the inner magnetosphere changes, expanding the region penetrated by energetic particles to lower latitudes. When a proton event occurs simultaneously with geomagnetic storms, communication failures in the HF band and radiation exposure of crew members aboard space stations and aircrafts occur across a wider region.

Acknowledgements

The author wishes to thank Prof. Tanaka of Kyushu University, Dr. Obara, the leader of the Space Simulation Group at CRL, Dr. Kikuchi of the Space Weather Group at CRL, and Dr. Kunitake, senior researcher at CRL, for valuable advice. The LASCO image data acquired by the SOHO satellite was provided by ESA and NASA; SXT image data of the Yohkoh satellite was provided by ISAS; data on PCN indices was provided by the Danish Meteorological Institute. Dst indices were provided by the World Data Center for Geomagnetism, Kyoto University. Solar wind data was taken by NASA Wind and ACE

satellites (MAG, SWEPAM). The author wishes to express his gratitude to all of the above organizations.

References

- 1 W. D. Gonzalez and B. T. Tsurutani, "Criteria of interplanetary parameters causing intense magnetic storms ($Dst < -100$ nT)", *Planet Space Sci.*, 35, 1101-1109, 1987.
- 2 K. Marubashi, "Interplanetary Magnetic Flux Ropes", This Special Issue of CRL Journal.
- 3 M. Sugiura and T. Kamei, "Equatorial Dst index 1957-1986", in IAGA Bulletin. 40, edited by A. Berthelier, and M. Menvielle, Int. Serv. of Geomagn. Indices Publ. Off., Saint Maur, France, 1991.
- 4 R. K. Burton, R. L. McPherron, and C. T. Russell, "An empirical relationship between interplanetary conditions and Dst", *J. Geophys. Res.*, 80, 4204-4214, 1975.
- 5 T. P. O'Brien and R. L. McPherron, "An empirical phase space analysis of ring current dynamics: Solar wind control of injection and decay", *J. Geophys. Res.*, 105, 7707-7719, 2000a.
- 6 A. J. Dessler and E. N. Parker, "Hydromagnetic theory of geomagnetic storms", *J. Geophys. Res.*, 64, 2239-2252, 1959.
- 7 N. Sckopke, "A general relation between the energy of trapped particles and the disturbance field over the Earth", *J. Geophys. Res.*, 71, 3125-3130, 1966.
- 8 T. Tanaka, "Generation of convection in the magnetosphere-ionosphere coupling system", This Special Issue of CRL Journal.
- 9 M. Sugiura and D. J. Poros, "A magnetospheric field model incorporating the OGO 3 and 5 magnetic field observations", *Planet. Space Sci.*, 21, 1763-1773, 1973.
- 10 I. A. Daglis, "The role of magnetosphere-ionosphere coupling in magnetic storm dynamics", *Magnetic Storms* edited by Tsurutani, B. T., Gonzalez, W. D., Kamide, Y., Arballo, J. K., 107-116, 1997.
- 11 M. Heinenman and R. A. Wolf, "Relationships of models of the inner magnetosphere to the Rice convection model", *J. Geophys. Res.*, 106, 15,545-15,554, 2001.
- 12 G. K. Parks, *Physics of Space Plasmas*, Addison-Wesley Publishing Company, 1991.
- 13 V. O. Papitashvili, N. E. Papitashvili, and J. H. King, "Solar cycle effects in planetary geomagnetic activity: Analysis of 36-year long OMNI dataset", *Geophys. Res. Lett.*, 27, 2797-2800, 2000.
- 14 Y. I. Feldstein, Modeling of the magnetic field of magnetospheric ring current as a function of interplanetary medium parameters, *Space Sci. Rev.*, 59, 83-165, 1992.
- 15 S. Watanabe, E. Sagawa, K. Ohtaka and H. Shimazu, "The response of geomagnetic storm index Dst to the solar wind parameters: Researched by a neural network method", submitted to *Earth, Planets and Space*.
- 16 Y. Kamide, "Is substorm occurrence a necessary condition for a magnetic storm?", *J. Geomagn. Geoelectr.*, 44, 109-117, 1992.
- 17 T. W. Hill, "Magnetic merging in a collisionless plasma", *J. Geophys. Res.*, 80, 4689-4699, 1975.
- 18 B. U. O. Sonnerup, "Magnetopause reconnection rate", *J. Geophys. Res.*, 79, 1546-1549, 1974.
- 19 T. W. Hill, A. J. Dessler, and R. A. Wolf, "Mercury and Mars: The role of ionospheric conductivity in the acceleration of magnetospheric particles", *Geophys. Res. Lett.*, 3, 429-432, 1976.
- 20 G. L. Siscoe, G. M. Erickson, B.U. O. Sonnerup, N. C. Maynard, J. A. Schoendorf, K. D. Siebert, D. R. Weimer, W. W. White, and G. R. Wilson, "Hill model of transpolar potential saturation: Comparisons with MHD simulations", *J. Geophys. Res.*, 107(A6), 10.1029/2001JA000109, 2002.

- 21 O. A. Troshichev, V. G. Andersen, S. Vennerstrom, and E. Friis-Christensen, "Magnetic Activity in the Polar Cap -A New Index", *Planet. Space Sci.*, 36, 1095-1102, 1988.
- 22 O. A. Troshichev, H. Hayakawa, A. Matsuoka, T. Mukai, and K. Tsuruda, "Cross polar cap diameter and voltage as a function of PC index and interplanetary quantities", *J. Geophys. Res.*, 101, 13,429-13,435 1996.
- 23 T. Nagatsuma, "Saturation of polar cap potential by intense solar wind electric fields", *Geophys. Res. Lett.*, 29(10), 10.1029/2001GL014202, 2002.
- 24 J. R. Wygant, D. Rowland, H. Singer, M. Temerin, F. Mozer, M. K. Hudson, "Experimental evidence on the role of the large spatial scale electric field in creating the ring current", *J. Geophys. Res.*, 103, 29,527-29,544, 1998.
- 25 T. Obara, M. Den, Y. Miyoshi, and A. Morioka, "Energetic Electron Variation in the Outer Radiation Zone During Early May 1998 Magnetic Storm", *J. Atmos. Sol. Terr. Phys.*, 62, 1405-1412, 2000.
- 26 J. E. Borovsky, M. F. Thomsen, and D. J. McComas, "The superdense plasma sheet: Plasmaspheric origin, solar wind origin, or ionospheric origin?", *J. Geophys. Res.*, 102, 22,089-22,097, 1997.
- 27 T. Terasawa, M. Fujimoto, T. Mukai, I. Shinohara, Y. Saito, T. Yamamoto, S. Machida, S. Kokubun, A. J. Lazarus, J. T. Steinberg, and R. P. Lepping, "Solar wind control of density and temperature in the near-earth plasma sheet: WIND/GEOTAIL collaboration", *Geophys. Res. Lett.*, 24, 935-938, 1997.
- 28 Y. Ebihara and M. Ejiri, "Modeling of solar wind control of the ring current buildup: A case study of the magnetic storm in April 1997", *Geophys. Res. Lett.*, 25, 3751-3754, 1998.
- 29 T. P. O'Brien and R. L. McPherron, "Evidence against an independent solar wind density driver of the terrestrial ring current", *Geophys. Res. Lett.*, 27, 3797-3800, 2000b.
- 30 S. Chapman, "Earth storms: retrospect and prospect", *J. Phys. Soc. Jpn.*, 17, suppl. A-I, 6-16, 1962.
- 31 T. Iyemori and D. R. K. Rao, "Decay of the Dst field of geomagnetic disturbance after substorm onset and its implication to storm-substorm relation", *Ann. Geophys.*, 14, 608-618, 1996.
- 32 S. Ohtani, Nose, M., Rostoker, G., Singer, H., Lui, A.T. Y., and Nakamura, M., "Storm-substorm relationship: Contribution of the tail current to Dst", *J. Geophys. Res.*, 106, 21,199-21,210, 2001.
- 33 Reeves, G. D. et al., "IMAGE, POLAR, and geosynchronous observations of substorm and ring current ion injection", in press.
- 34 Y. Ebihara, "Numerical simulations on the dynamics of charged particles in the inner magnetosphere associated with a magnetic storm", Ph.D thesis, 1999.
- 35 W. Baumjohann, Y. Kamide, and R. Nakamura, "Substorms, storms, and the near-Earth tail", *J. Geomagn. Geoelectr.*, 48, 177-185, 1996.
- 36 T. Ondoh and K. Marubashi, (Eds.), "Science of Space Environment", Ohm-sha, 2000.
- 37 I. A. Erinmez, S. Majithia, C. Rogers, T. Yasuhiro, S. Ogawa, H. Swahn, and J. G. Kappenman, "Application of modeling techniques to assess geomagnetically induced current risks on the NGC transmission system".
- 38 T. Obara, "Formation of the Magnetosphere and Magnetospheric Plasma Regime", This Special Issue of CRL Journal.



NAGATSUMA Tsutomu, Ph. D.

*Senior Researcher, Space Weather
Group, Applied Research and Stand-
ards Division*

Solar-Terrestrial Physics